Sensors & Transducers, Vol. 176, Issue 8, August 2014, pp. 83-87

Sensors & Transducers

The Sum-frequency Effect of Antiferromagnetic Sandwich Structure

[1, 2] Hong Liang, [3] Shu-Fang Fu, [3] Sheng Zhou, [3] Xuan-Zhang Wang
[1] Department of Dielectric Engineering, Harbin University of Science and Technology, Harbin 150080, China
[2] Department of Physics, Harbin University, Harbin 150086, China
[3] School of Physics and Electronic Engineering, Harbin Normal University, Harbin 150025, China
[1] Tel.: 15045803688
[1] E-mail: lghrb@sina.com

Received: 2 July 2014 /Accepted: 4 August 2014 /Published: 31 August 2014

Abstract: A new way to increase the sum-frequency generation based on the antiferromagnetic sandwich structure in the THz frequency field is presented. We find that the SF outputs near the higher resonant frequencies are stronger than those near the lower ones and the effect of the dielectric on sum-frequency outputs also is discussed. *Copyright © 2014 IFSA Publishing, S. L.*

Keywords: Sum-frequency generation, Antiferromagnetic sandwich structure, THz frequency field, Sum-frequency output, Resonant frequencies.

1. Introduction

The sum-frequency (SF) generation technique is widely used as one method of frequency conversion [1-3]. In the conversion process, light of two frequencies is mixed in a nonlinear crystal, resulting in the generation of new light sources at the sum or difference frequency. In recent years, the nonlinearities of antiferromagnets (AFs) have been paid a great deal of attention to, for example, the second-harmonic generation [4-6]. In addition, the resonant frequencies of typical AF materials are distributed over the far-infrared and millimeter ranges [7-9], so their nonlinearity is of practical interest in these ranges. However, a very strong electromagnetic wave is needed to illuminate AFF in order to induce the nonlinearity of AFF since the AF nonlinearity is weak. Wang [10-11] presented a method to increase the second-harmonic generation (SHG) by an AFF for a fixed input power, in which the film is put between two different dielectrics or in one-dimensional photonic crystals. The results show that the SH outputs are raised to a few hundred times that of the single film. The SF outputs of a single AF film has been discussed by Fu [12], an optimum interact length is defined. However, the SF outputs, the second-nonlinear response of AF, are much weaker, which lead to the lower SF conversion efficiency. In this paper, AF sandwich structure is considered. Comparing with the SF outputs of AF film, the ones obtained in this paper near the higher resonant frequency will be increased about 5 times. The effect of the dielectric also is discussed.

2. Theoretical Model and Formalism

As illustrated in Fig. 1, we concentrate our attention on the case where the external magnetic field and AF anisotropy axis both are along the z axis and parallel to layers. Two linearly polarized radiations are obliquely incident on the upper surface.

I_l, R_l and T_l indicate the incident, reflection and transmission waves, respectively, with the incident angle θ_l and transmission angle θ_l' (l=1or2). T_n^a and T_n^b represent the corresponding output quantities of SF waves with direction angles θ_n and θ_n'. The two signal waves in the film are not indicated in Fig. 1. The SF magnetization arises as a source term in the SF wave equations and is excited by the pump waves, and in turn the pumping waves are induced by the incident waves.

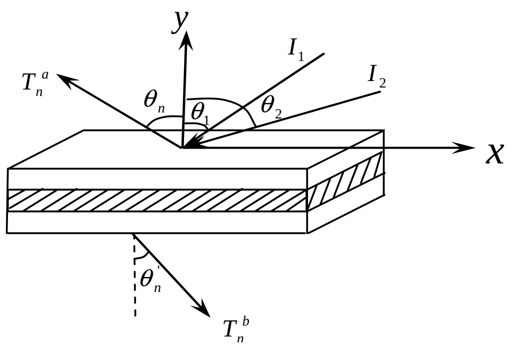

Fig. 1. Geometry and coordinate system.

$$E_{lz} = \exp(ik_{lx}x - i\omega_l t)\times$$
$$\times\begin{cases} I_{l0}\exp(ik_{l0}y) + \mathrm{R}_{l0}\exp(-ik_{l0}y), & \text{(in the above space)} \\ A_{lj}\exp(ik_{lj}y) + B_{lj}\exp(-ik_{lj}y), & \text{(in the j-layer)} \\ T_{l0}\exp(ik_{l0}y), & \text{(in the below space)} \end{cases} \tag{1}$$

where the subscript l =1 or 2 described the two pump waves, and j=1, 2, or a described the dielectric and AFF layers, respectively. The wave-number components $k_0 = [(\omega/c)^2 - k_{lx}^2]^{1/2}$, $k_1 = [\varepsilon_1(\omega/c)^2 - k_{lx}^2]^{1/2}$, $k_2 = [\varepsilon_2(\omega/c)^2 - k_{lx}^2]^{1/2}$ and $k_a = [\varepsilon_a\mu_v(\omega/c)^2 - k_{lx}^2]^{1/2}$ with $k_{lx} = (\omega/c)\sin\theta$ and the AF effective permeability $\mu_v = (\mu_{xx}^2 + \mu_{xy}^2)/\mu_{xx}$. The capital characters on the right side of (5) represent the wave amplitudes in different spaces, where I_0 and R_0 as well as T_0 are related to the incident, reflection and transmission waves, respectively. In terms of $i\omega\mu_0(1+\vec{\chi})\cdot\vec{H} = \nabla\times\vec{E}$, the corresponding magnetic fields in different spaces are written.

Using the matrix method, we obtain the matrix equation satisfied by the reflection, transmission and incident amplitudes in the linear situation,

$$\begin{pmatrix} I_{l0} \\ R_{l0} \end{pmatrix} = T_{t1}T_{1a}T_{a2}T_{2b}\begin{pmatrix} T_{l0} \\ T_{l0} \end{pmatrix}, \tag{2}$$

$$T_{t1} = \frac{1}{2k_0}\begin{pmatrix} k_0 + k_l & k_0 - k_l \\ k_0 - k_l & k_0 + k_l \end{pmatrix}, \tag{3a}$$

$$T_{1a} = \frac{1}{2}\begin{pmatrix} (1+\delta_{l1}^{+})\exp(-ik_{l1}d_1) & (1-\delta_{l1}^{-})\exp(-ik_{l1}d_1) \\ (1-\delta_{l1}^{+})\exp(ik_{l1}d_1) & (1+\delta_{l1}^{-})\exp(ik_{l1}d_1) \end{pmatrix}, \tag{3b}$$

$$T_{a2} = \frac{\mu_v(\omega_l)k_{l2}}{2k_{la}}\begin{pmatrix} (\delta_{l2}^{-}+1)\exp(-ik_{la}d_a) & (\delta_{l2}^{-}-1)\exp(-ik_{la}d_a) \\ (\delta_{l2}^{+}-1)\exp(ik_{la}d_a) & (\delta_{l2}^{+}+1)\exp(ik_{la}d_a) \end{pmatrix} \tag{3c}$$

$$T_{2b} = \frac{1}{2k_{l2}}\begin{pmatrix} (k_{l2}+k_{l0})\exp(-ik_{l2}d_2) & 0 \\ 0 & (k_{l2}-k_{l0})\exp(ik_{l2}d_2) \end{pmatrix}, \tag{3d}$$

$$\delta_{l1,2}^{\pm} = (k_{la} \pm k_{lx}\mu_{xy}(\omega_l)/\mu_{xx}(\omega_l))/(\mu_v(\omega_l)k_{l1,2}) \tag{4}$$

The pumping amplitudes can be solved from equation (2), which can be described as

$$\begin{pmatrix} I_{l0} \\ R_{l0} \end{pmatrix} = T_{t1}T_{1a}\begin{pmatrix} A_{la} \\ B_{la} \end{pmatrix} \tag{5}$$

It is well known that SF waves are the second-order nonlinear response of AFF. For TE waves, there is only one equation which contains a source term in the three components equations of the nonlinear wave equation. It is presented as

$$-\left(\frac{\partial^2}{\partial x^2} + \frac{\partial^2}{\partial y^2}\right)H_{nz}(\omega_n) - \varepsilon_a(\omega_n/c)^2 H_{nz}(\omega_n) = \varepsilon_a(\omega_n/c)^2\vec{m}_z^{(2)}(\omega_n) \tag{6}$$

In the equation, $\vec{m}_z^{(2)}(\omega_n)$ is the second-order magnetization presented by

$$\begin{aligned} \vec{m}_z^{(2)}(\omega_n) = {} & \chi_{xzz}(H_{1x}(\omega_1)H_{2x}(\omega_2) + H_{1y}(\omega_1)H_{2y}(\omega_2)) \\ & + \chi_{zxy}(H_{1x}(\omega_1)H_{2y}(\omega_2) - H_{1y}(\omega_1)H_{2x}(\omega_2)) \end{aligned} \tag{7}$$

with $\omega_n = \omega_1 + \omega_2$. The nonzero expression of the second-order can be found in the reference[12]. Let

$$\begin{aligned} H_{nz}(\omega_n) = {} & [A_{na}e^{ik_{nay}y} + B_{na}e^{-ik_{nay}y} + \\ & + N_1 e^{i(k_{1ay}+k_{2ay})y} + N_2 e^{-i(k_{1ay}+k_{2ay})y} + \\ & + N_3 e^{i(k_{2ay}-k_{1ay})y} + N_4 e^{-i(k_{2ay}-k_{1ay})y}]e^{(ik_{nx}x - i\omega_n t)}, \end{aligned} \tag{8}$$

where $k_{nay} = [\varepsilon_a\mu_v(\omega_n/c)^2 - k_{nx}^2]^{1/2}$ with $k_{nx} = k_{1x} + k_{2x}$. The nonlinear coefficient can be written as

$$N_1 = \varepsilon_a\omega_n^2 F^{+}[\chi_{xzz}(\Delta_1^{+}\Delta_2^{+} + \Delta_1'^{-}\Delta_2'^{-}) + \chi_{zxy}(\Delta_1'^{-}\Delta_2^{+} - \Delta_1^{+}\Delta_2'^{-})]A_{1a}A_{2a} \tag{9a}$$

$$N_2 = \varepsilon_a\omega_n^2 F^{+}[\chi_{xzz}(\Delta_1^{-}\Delta_2^{-} + \Delta_1'^{+}\Delta_2'^{+}) + \chi_{zxy}(\Delta_1^{-}\Delta_2'^{+} - \Delta_1'^{+}\Delta_2^{-})]B_{1a}B_{2a} \tag{9b}$$

$$N_3 = \varepsilon_a\omega_n^2 F^{-}[\chi_{xzz}(\Delta_1'^{+}\Delta_2'^{-} - \Delta_1^{-}\Delta_2^{+}) + \chi_{zxy}(\Delta_1^{-}\Delta_2'^{-} + \Delta_1'^{+}\Delta_2^{+})]A_{2a}B_{1a} \tag{9c}$$

$$N_4 = \varepsilon_a\omega_n^2 F^{-}[\chi_{xzz}(\Delta_1'^{-}\Delta_2'^{+} - \Delta_1^{+}\Delta_2^{-}) - \chi_{zxy}(\Delta_1^{+}\Delta_2'^{+} + \Delta_1'^{-}\Delta_2^{-})]A_{1a}B_{2a} \tag{9d}$$

here

$$F^{\pm} = \frac{1}{\omega_1\omega_2\mu^2{}_0\mu_{2v}(\omega_2)\mu_{1v}(\omega_1)\mu_1(\omega_2)\mu_1(\omega_1)\delta^{\pm}}, \quad (10a)$$

$$\delta^{\pm} = (k_{2a} \pm k_{1a})^2 + (k_{1x} + k_{2x})^2 - \varepsilon_a\omega_n^2, \quad (10b)$$

$$\Delta_l^{\pm} = \mu_1(\omega_l)k_{lay} \pm i\mu_2(\omega_l)k_{lx}, \quad (10c)$$

$$\Delta_l'^{\pm} = \mu_1(\omega_l)k_{lx} \pm i\mu_2(\omega_l)k_{lay} \quad (10d)$$

We use $H_{nz}^a = T_n^a e^{-ik_{ny}y}e^{(ik_{nx}x - i\omega_n t)}$ to present the magnetic field of the SF wave generated above the film and $H_{nz}^b = T_n^b e^{ik_{ny}y}e^{(ik_{nx}x - i\omega_n t)}$ to indicate the SF field below, with k_{ny} determined by $k_{ny}^2 + k_{nx}^2 = \varepsilon_0(\omega_n / c)^2$. The SF electric fields in different spaces from $-i\omega_n\varepsilon_0\varepsilon_a\vec{E}_n = \nabla \times \vec{H}_n$ are found. Considering the boundary conditions of these fields to be continuous at the surface, there must be $k_{nx} = k_{1x} + k_{2x}$. The matrix equation between the layer`s amplitudes can be got from the boundary continuous condition. The magnetic amplitudes of the outputs can be solved from the equations as follows:

$$\begin{pmatrix} 0 \\ T_n^a \end{pmatrix} = M_{t1}[M_{1a}(M_{a2}M_{2b}\begin{pmatrix} T_n^b \\ T_n^b \end{pmatrix} + \Gamma_2) + \Gamma_1], \quad (11)$$

where

$$M_{1a} = \frac{1}{2k_{n1}\varepsilon_a}\begin{pmatrix} (k_{n1}\varepsilon_a - k_{nay}\varepsilon_1)\exp(-ik_{n1}d_1) & (k_{n1}\varepsilon_a + k_{nay}\varepsilon_1)\exp(-ik_{n1}d_1) \\ (k_{n1}\varepsilon_a + k_{nay}\varepsilon_1)\exp(ik_{n1}d_1) & (k_{n1}\varepsilon_a - k_{nay}\varepsilon_1)\exp(ik_{n1}d_1) \end{pmatrix} \quad (12a)$$

$$\Gamma_1 = \frac{1}{2}\begin{pmatrix} [(1-\eta^+)N_1 + (1+\eta^+)N_2 + (1-\eta^-)N_3 + (1+\eta^-)N_4]\exp(-ik_{n1}d_1) \\ [(1+\eta^+)N_1 + (1-\eta^+)N_2 + (1+\eta^-)N_3 + (1-\eta^-)N_4]\exp(ik_{n1}d_1) \end{pmatrix} \quad (12b)$$

$$T_{a2} = \frac{1}{2k_{nay}\varepsilon_2}\begin{pmatrix} e^{-ik_{nay}d_a}(k_{nay}\varepsilon_2 - \varepsilon_a k_{n2}) & e^{-ik_{nay}d_a}(k_{nay}\varepsilon_2 + \varepsilon_a k_{n2}) \\ e^{ik_{nay}d_a}(k_{nay}\varepsilon_2 + \varepsilon_a k_{n2}) & e^{ik_{nay}d_a}(k_{nay}\varepsilon_2 - \varepsilon_a k_{n2}) \end{pmatrix} \quad (12c)$$

$$\Gamma_2 = \frac{1}{2}\begin{pmatrix} [-(1+\upsilon^+)e^{i(k_{1ay}+k_{2ay})d_a}N_1 - (1-\upsilon^+)e^{-i(k_{1ay}+k_{2ay})d_a}N_2 - (1+\upsilon^-)e^{i(k_{2ay}-k_{1ay})d_a}N_3 - (1-\upsilon^-)e^{-i(k_{2ay}-k_{1ay})d_a}N_4]e^{-ik_{nay}d_a} \\ [-(1-\upsilon^+)e^{i(k_{1ay}+k_{2ay})d_a}N_1 - (1+\upsilon^+)e^{-i(k_{1ay}+k_{2ay})d_a}N_2 - (1-\upsilon^-)e^{i(k_{2ay}-k_{1ay})d_a}N_3 - (1+\upsilon^-)e^{-i(k_{2ay}-k_{1ay})d_a}N_4]e^{ik_{nay}d_a} \end{pmatrix} \quad (12d)$$

$$M_{t1} = \frac{1}{2k_{n0}\varepsilon_1}\begin{pmatrix} k_{n0}\varepsilon_1 - k_{n1} & k_{n0}\varepsilon_1 + k_{n1} \\ k_{n0}\varepsilon_1 + k_{n1} & k_{n0}\varepsilon_1 - k_{n1} \end{pmatrix}, \quad (13)$$

$$M_{2b} = \frac{1}{2k_{n2}}\begin{pmatrix} (k_{n2} - \varepsilon_2 k_{n0})\exp(-ik_{n2}d_2) & 0 \\ 0 & (k_{n2} + \varepsilon_2 k_{n0})\exp(ik_{n2}d_2) \end{pmatrix}. \quad (14)$$

According to the definition, the incident electromagnetic energy-flux density in the nonmagnetic materials is written as $S_{Il} = (\varepsilon_0^2 / \mu_0)^{1/2}|E_{0l}|^2 / 2$, but SF output densities are expressed as $S_a = (\mu_0 / \varepsilon_0^2)^{1/2}|T_a|^2 / 2$ for the above space of AFF and $S_b = (\mu_0 / \varepsilon_0^2)^{1/2}|T_b|^2 / 2$ for the below space of it.

3. Numerical Examples

We take a $SiO_2/MnF_2/ZnF_2$ sandwich structure as an example for numerical calculations, where the physical parameters: the dielectric constant $\varepsilon_a = 5.5$, the sublattice magnetization $M_0 = 0.6kG$ and the damping coefficient $\tau = 0.001$; the exchange field $H_e = 550kG$, anisotropy field $H_a = 7.87kG$ and the gyromagnetic ratio $\gamma = 1.97\times10^{10} rads^{-1}kG^{-1}$, leading to the resonant frequencies $\omega_1/2\pi c = 9.76cm^{-1}$ and $\omega_2/2\pi c = 9.86cm^{-1}$ in the external field of $H_0 = 1.0kG$. The thickness of AF film is taken to be $109\mu m$, $209\mu m$ for SiO_2 and $502\mu m$ for ZnF_2.

Fig. 2 and Fig. 3 illustrate the SF output densities S_a and S_b versus the frequency ω_n and the incident angle θ_1 of the signal wave when the other incident angle is fixed at $\theta_2 = 30^o$ with the fixed frequencies $\omega_2 = 9.70cm^{-1}$ and $\omega_2 = 9.85cm^{-1}$ which are near the two resonant frequencies of AFF. The highest S_a and S_b have been marked with ω_n and θ_1 in the figures. It can be seen that the highest SF outputs are located in the small incident angle region which can be understood that most incident can participate the process of generate the SF outputs. Obviously, the SF outputs on the below surface is more than those on the upper surface by one order. According to the SF $\omega_n = 19.51cm^{-1}$, the first incident wave frequency is $\omega_1 = 9.81cm^{-1}$ which is near the second resonant frequency. Evidently, in terms of their respective maxima the SF outputs on the above surface near the second frequency will be stronger on order than those near the first frequency.

Next we discuss the effect of the incident angle on S_a and S_b at $\omega_1 = \omega_2 = 9.75cm^{-1}$ and $\omega_1 = \omega_2 = 9.85cm^{-1}$ illustrated in Fig. 4 and Fig. 5, respectively. The maxima of S_a and S_b have been shown in the figures. It is apparent to be seen from the marks that the highest S_a and S_b are detected when the two signal waves are both in the region of $\theta < 30^0$ for $\omega_1 = \omega_2 = 9.75cm^{-1}$, however, $\theta > 30^0$ for $\omega_1 = \omega_2 = 9.85cm^{-1}$. With the increasing the incident angles the SF outputs will dramatically decrease when the $\theta > 60^0$, which can be understood that most input flux-energy will be reflected by the above surface film. The flux-energy left in the film cannot induce the SF outputs since the second-order nonlinear response of AFF is induced by a strong electro- magnetic wave. It is obvious that the SF outputs near the second resonant frequency are much stronger than those near the first resonant frequency.

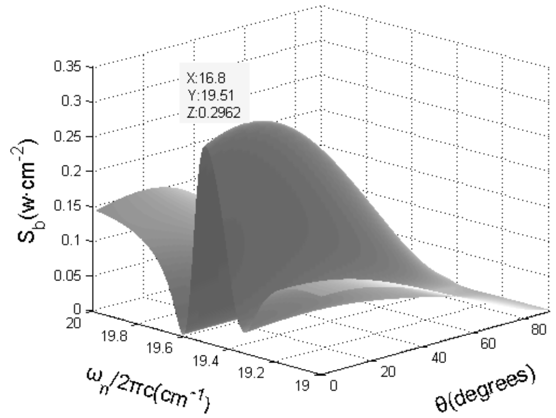

Fig. 2. S_a and S_b versus the incident angle θ_1 and the SF frequency ω_n at $\omega_2 = 9.70cm^{-1}$ and $\theta_2 = 30^o$ for $SiO_2/MnF_2/ ZnF_2$.

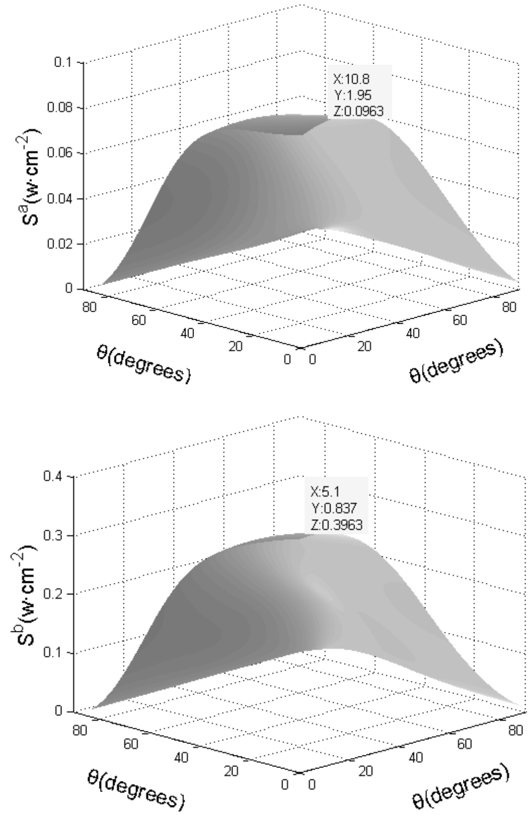

Fig. 4. S_a and S_b versus θ at $\omega_1 = \omega_2 = 9.75cm^{-1}$ for $SiO_2/MnF_2/ ZnF_2$.

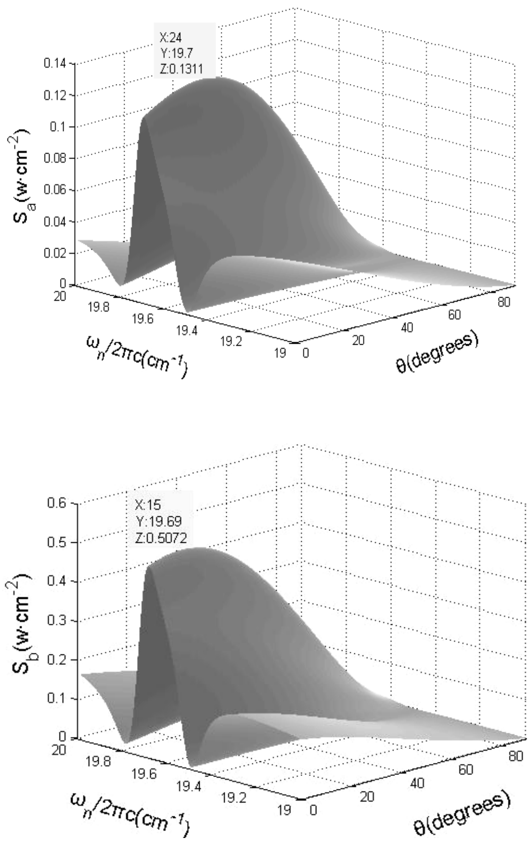

Fig. 3. S_a and S_b versus θ_1 and ω_n at $\omega_2 = 9.85cm^{-1}$ and $\theta_2 = 30^o$ for $SiO_2/MnF_2/ ZnF_2$.

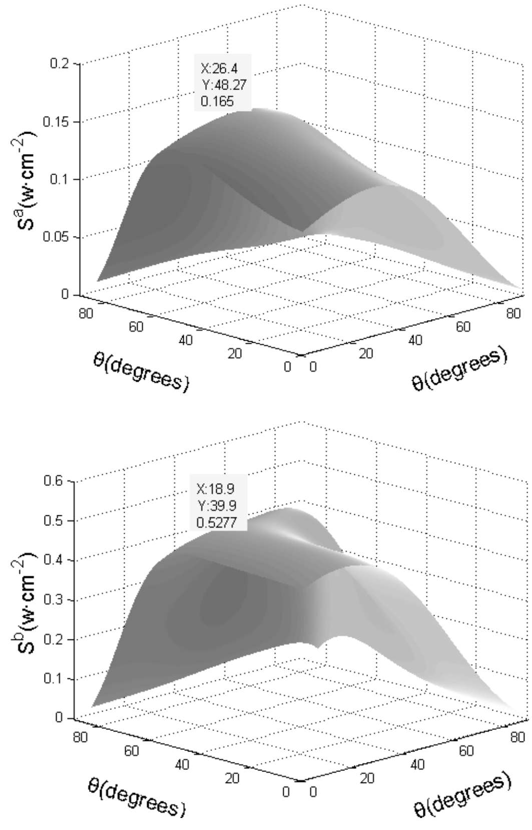

Fig. 5. S_a and S_b versus θ at $\omega_1 = \omega_2 = 9.85cm^{-1}$ for $SiO_2/MnF_2/ ZnF_2$.

In order to investigate the effect of the dielectric on the SF outputs, the Fig. 6 shows S_a and S_b versus the incident angles at $\omega_1 = \omega_2 = 9.75 cm^{-1}$ for $ZnF_2/MnF_2/SiO_2$. Comparing with Fig. 4 and Fig. 5, the SF outputs in this case are much weaker since the dielectric of ZnF_2 is bigger than that of MnF_2.

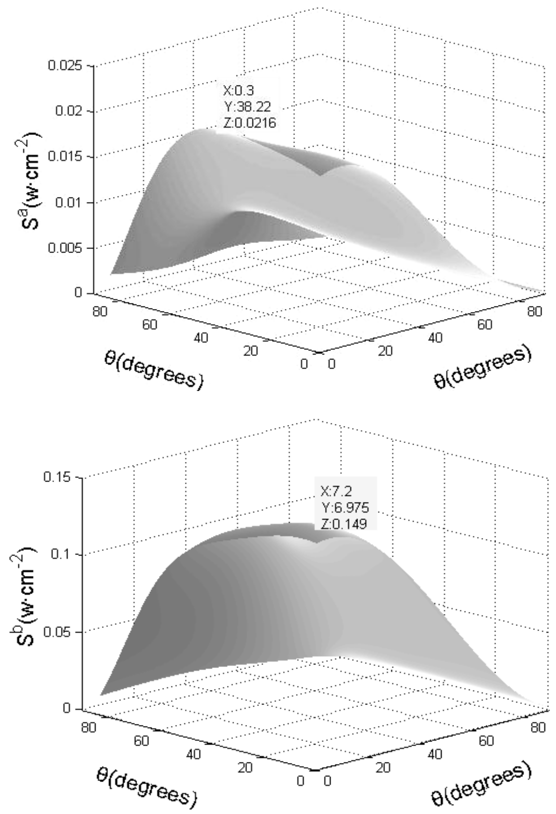

Fig. 6. S_a and S_b versus θ_1 and θ_2 at $\omega_1 = \omega_2 = 9.75 cm^{-1}$ for $ZnF_2/MnF_2/SiO_2$.

4. Summary

In this paper, the SF generation of $SiO_2/MnF_2/ZnF_2$ has been investigated through the matrix method in THz frequency field. We found that the highest SF outputs are suited at the small incident angle regions since the nonlinear response needs more power to be induced. It is well known that more incident energy is transported into the film to attend the process of generating SF outputs at the small incident angles. The SF outputs on the below surface are much stronger than those on the above film. In addition, an optimum dielectric/AF/dielectric is discussed. Choosing the proper incident frequencies and the angles will benefit to the SF generation in the THz frequency field.

Acknowledgment

This work was supported financially by the Science and technology project of Education Commission Heilongjiang Province through grant12523033, it is also supported by the National Natural Science Foundation of China through grant 11104050, also by the National Nature Science Foundation of China through grant 11204056.

References

[1]. E. Mimoun, L. D. Sarlo, J.-J. Zondy, J. Dalibard, F. Gerbier, Sum-frequency generation of 589 nm light with near-unit efficiency, *Opt. Express*, 16, 2008, pp. 18684-18690.

[2]. J. D. Vance, C. Y. She, H. Moosmuller, Continuous-wave, all-solid-state, single-frequency 400-mw source at 589 nm based on doubly resonant sum-mixing in a monolithic lithium niobateresonantor, *Appl. Opt.*, 37, 1998, pp. 4891-4896.

[3]. T. H. Jeys, A. A. Brailove, A. Mooradian, Sum frequency generation of sodium resonance radiation, *Appl. Opt.*, 28, 1989, pp. 2588-2591.

[4]. M. Fiebig, D. Frohlich, B. B. Krichevtsov, R. V. Pisarev, Second harmonic generation and magnetic-dipole-electric-dipole interference in antiferromagnetic Cr_2O_3, *Phys. Rev. Lett.*, 73, 1994, pp. 2127-2130.

[5]. S. C. Lim, Second harmonic generation of magnetic and dielectric multilayers, *J. Phys.: Condens. Matter*, 18, 2006, pp. 4329-4343.

[6]. M. Fiebig, D. Frohlich, T. Lottermoser, R. V. Pisarev, H. J. Weber, Second harmonic generation in the centrosymmetric antiferromagnet NiO, *Phys. Rev. Lett.*, 87, 2001, pp. 137202.

[7]. K. Abraha, D. R. Tilley, Theory offar infrared properties of magnetic surfaces, films and superlattices, *Surf. Sci. Rep.*, 24, 1996, pp. 125–222.

[8]. Z. Yan, S.-F. Fu, H. Li and X.-Z. Wang, Nonlinear Far-Infrared Transmission of Antiferromagnetic Fabry-Perot Resonator, *IEEE Transactions on Magnetics*, Vol. 48, Issue 4, April 2012, pp. 1597-1600.

[9]. D.-M. Sun, S.-F. Fu, S. Zhou, X.-Z. Wang, Numerical simulation of optical bi-stability in antiferromagnetic sandwich structure, *J. Magn. Magn. Materials*, 324, 2012, pp. 183-189.

[10]. S. Zhou and X.-Z. Wang, Method of enhancing second-harmonic generation of Antiferromagnetic film, *J. Opt. Soc. Am.* B 25, 2008, pp. 1639-1644.

[11]. S. Zhou, H. Li, S.-F. Fu, X.-Z. Wang, Second harmonic generation from an Antiferromagnetic film in one-dimensional photonic crystals, *Phy. Rev*. B, 80, 2009, pp. 205409.

[12]. Shufang Fu, Sheng Zhou, Hong Liang, Xuan-Zhang Wang, Phase-matched sum frequency generation of antiferromagnetic film in THz frequency field, *J. Magn. Magn. Materials*, 346, 2013, pp. 178-185.